



A LIGHT SCATTERING METHOD TO MEASURE REAL-TIME PARTICULATE EMISSIONS

Rose Gong, Keryn Williams

¹ School of Chemical and Physical Sciences, Victoria University of Wellington,
PO Box 600, Wellington, New Zealand.

1. ABSTRACT

Dynamic analysis of particulate emissions from vehicles has been a challenge. A dynamic particulate measurement method applying light scattering theory is being developed at Victoria University. A particle model has to be set to apply light scattering theory. To simplify the problem, a Fraunhofer diffraction model has been used. The scattered light intensities have been measured at different scattered angles from the particles in an exhaust stream with a lock-in amplifier system, and then the scattered light intensities were used in the model to solve the particle size distributions. Since the model equations are non-linear, analytical solutions cannot be obtained easily. The first dark ring theory was applied initially to overcome non-linearity. However this method over estimates small sized particles. To solve the non-linear equations, numerical calculations based on the least squares method were carried out. Firstly we worked on numerical calculations with the scattered light intensity-scattered angle profiles produced by a single detector measurement system. Different size groups have been chosen for the calculation. Reasonably good agreement was obtained with the different choices. Secondly, we modified the optical design of the light intensity measurement, in particular, for large angle area, which the scattered light is much weaker than that in the small angle area. Optical lenses were introduced in the system. This modified design has increased the signal quality of large-angle scattered light intensity significantly, and enables us to take real-time measurements from dynamic particulate emissions. However using lenses decreases the number of data points used in the numerical calculations.

2. INTRODUCTION

Particulate emissions from diesel vehicles have been recognised as a significant source of suspended particulate matter in the atmosphere. In urban areas the proportion of diesel particle matter in the atmospheric particulate matter is higher than non-urban areas, if the particulate matter from natural sources is excluded. For example, a report of U.S. EPA (Environmental Protection Agency) [1] showed that the estimated range of diesel PM_{2.5} contribution to the total inventory was from 10% to 32% in some urban areas in California, Colorado and Arizona. Diesel particulate emissions can have serious impacts on human health. Chambellan and colleagues [2] explained the effects of diesel particles on asthma and allergic rhinitis. Studies carried out in US [1, 3, 4] and in Europe [5] showed that diesel particles were related to respiratory diseases, in particular, lung cancer, and increased mortality and morbidity. The finer the particles, the larger the surface area where chemicals can attach, and the deeper they can penetrate into the respiratory system. Diesel exhaust particles can also contribute to climate change. The black carbon particles not only

have a water nucleation effect in the atmosphere causing increased cloud formation [6], but they might be partially responsible for the global warming effect as well, according to Jacobson's research [7].

Diesel particles are the products of incomplete combustion. Diesel particulate emission is one of the important parameters for engine performance and engine combustion efficiency. The physical characteristics of diesel particulate emissions vary under different operational conditions. For example, the particle size range and size distributions and the mass of diesel particles will change if an engine is running under different speeds or different loads. Particulate emissions from different types of diesel engines are very different. To understand the physical characters of diesel particles and how they change is very important for the analysis of engine performance and its efficiency and for the investigations of the relationship between particle size and the its effects on human health and climate changes. So it is vital to study the diesel particulate emissions as a function of vehicle type and engine operational conditions, particularly, transient operating conditions. The analysis of real-time measurements of diesel particulate emissions will reveal the function.

In recent years, much of the research work on diesel particulate emissions has been concentrated on real-time measurements. The real-time measurement of collective diesel particulate emissions has been carried out in a mountain tunnel reported by Cadle [8]. An instrument sampled the ambient air inside the tunnel continuously and measured the particle size. The characteristics of particulate matter (PM) emissions were different between heavy-duty diesel vehicles and light-duty diesel vehicles. Individual vehicle's real-time particulate measurements on a chassis dynamometer with a dilution tunnel fitted with isokinetic particulate sampling probes were reported by Moosmüller and colleagues [9], who used five different methods to measure PM mass in a driving cycle test. Experiments on a similar dynamometer testing facility with a photometer were carried out by Cheung [10] to measure the instant PM mass under defined speeds and transient operating conditions. Their results showed that PM mass varied with changes of vehicle speeds, and at the beginning of a speed change, the PM mass increased. However, the dilution tunnel sampling process could "smooth out" some sharp changes. Both the mass and size distribution of diesel PM exhaust will change if the vehicle operational condition changes. In order to observe the changes of particle size distribution immediately after the exhaust pipe, a light scattering method is being developed at Victoria University of Wellington, which will enable us to measure particulate emissions without disturbing them. It is critical to be able to measure particle size distributions remotely (open-path) directly from the exhaust pipe in order to understand the relationship of size distributions and engine performances. When exhausts are cooled down in air or in a dilution tunnel, there is a chance that volatile compounds will condense on the surfaces of the particles, and that particle aggregations could be encouraged. This paper explains the early stage of the development of this light scattering method, and discusses the results of different methods of calculating particle size distribution from the scattered light measurements

3. LIGHT SCATTERING

Particles scatter light when they are in a light beam. The pattern of scattered light intensity from a particle could be a function of incident light intensity, the wavelength of the incident light, scattering angle, the size and shape of the particle and the refractive index. If the scattered light from particles can be measured, the particle

size distribution can be obtained by applying the proper light scattering theory or model and an appropriate calculation method.

3.1 LIGHT SCATTERING FOR SMALL PARTICLES

There are different light scattering theories for different light scattering problems. In general, a particle scatters light as shown in Figure 1, where q is the scattering angle.

It can be described by equation (1) as given in reference [12]:

$$I = \frac{I_o F(q, j)}{k^2 r^2}, \quad (1)$$

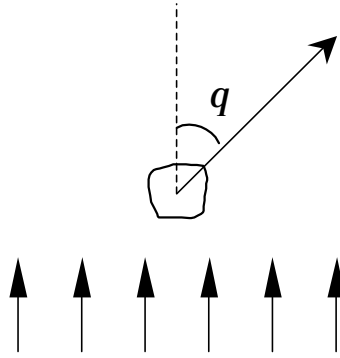


Figure 1 A particle scatters light

where I_o is the intensity of incident light, I is the intensity of scattered light at a point, which is at a large distance r from the particle, and k is the wave number defined by $k = 2\pi/\lambda$, where λ is the wavelength of the light. $F(q, j)$ is a dimensionless function of the direction of scattering, in which j is an azimuth angle. It also depends on the orientation of the particle with respect to the incident light and on the

state of polarisation of the incident light. $F(q, j)$ can be defined in different forms to deal with different scattering problems.

The classic method to describe the scattering by a particle, whose size is in the same magnitude as λ , or larger than λ , is Mie scattering theory. In Mie scattering, scattered light will be examined in two wave planes perpendicular to each other, and the amplitudes of the components of the scattered light are the function of the orientations of detecting of scattering in the two planes, the physical appearance of the particle, i.e. the shape and size, and the composition of the particle, i.e. the refractive index.

To apply Mie theory to diesel particle emissions is complex. Based on the research budget of this project, a modified simple scattering model has been chosen to test the principle of measuring the size distributions of dynamic particles remotely, before the more sophisticated Mie theory is used.

3.2 OUR MODEL

The model we used is not an accurate description of a real diesel particle. The electronic microscope image of real diesel particles is shown in Figure 2. Our model describes an idealised particle with a similar physical effect to the real one. We treated the diesel particles as:

- Particles from the exhaust are homogenous spheres;
- The sizes of the particles are much greater than the wavelength of the incident light;
- The incident light is unpolarised light;
- There is sufficient room between particles, so the scattering pattern of each individual particle is undisturbed by the presence of other particles;

- The thickness of the exhaust cloud in the laser beam is so small compared with the distance between the exhaust and the detector that the thickness is negligible. All of the scattering sources come from the same origin.

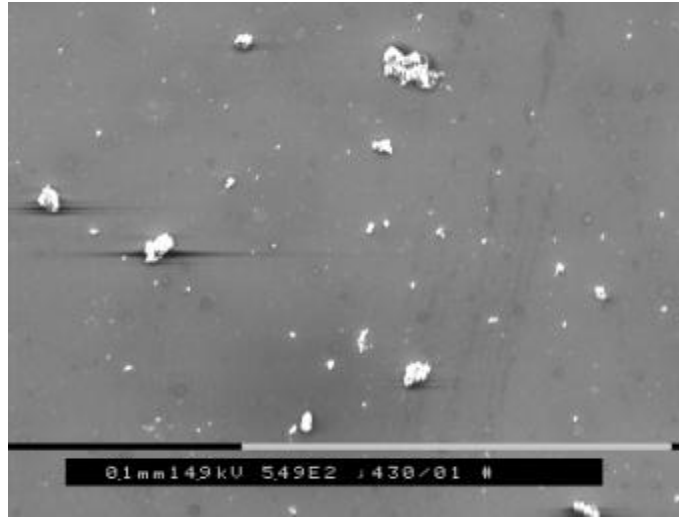


Figure 2 Electronic microscope image of diesel particles

Light scattering of our model then can be described by Fraunhofer diffraction as explained by van de Hulst [12]. The light scattering pattern of a single particle described by Fraunhofer diffraction theory is shown as,

$$I_r(a, q) = \frac{I(a, q)}{I_o} = \frac{\left| x^2 \frac{J_1(x \sin q)}{x \sin q} \right|^2}{k^2 r^2} \quad (2)$$

where $k = 2\pi / \lambda$, and $x = ka$.

- I_r : Relative intensity of scattered light;
- I : Intensity of scattered light;
- I_o : Intensity of incident light;
- λ : Wavelength of the incident light;
- r : Distance from the particle to the detector;
- a : Radius of the particle;
- q : Scattering angle;
- J_1 : Bessel function (1st order).

In a diesel exhaust cloud, there are N_i particle with radius a_i . $N(a_i)$ is the particle size distribution of the diesel exhaust, and the total scattered light of the exhaust particles at scattering angle q is

$$I_q = \sum_i I_r(a_i, q) \cdot N(a_i). \quad (3)$$

$s(q)$ is the measured scattered light intensity signal at q , then

$$s(q) = I_q = \sum_i I_r(a_i, q) \cdot N(a_i). \quad (4)$$

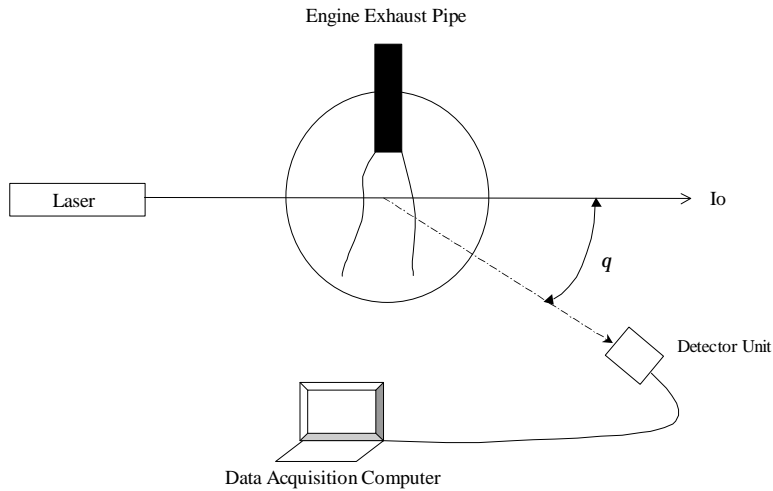
If the scattered light intensity is measured at n scattering angles, the following set of equations can be obtained:

$$s(q_j) = I_q = \sum_i I_r(a_i, q_j) \cdot N(a_i), \quad j = 1, 2, \dots, m. \quad (5)$$

a_i and $N(a_i)$ are both unknown, so equations (5) are a set of nonlinear equations. Once those equations are solved, the particle distributions will be obtained.

3.3 FIRST LIGHT SCATTERING EXPERIMENT

A laser – lock-in amplifier detecting system was built to work with a VM 292 two-cylinder diesel engine to measure the scattered light from diesel exhaust as it was described in our earlier paper [11], and its schematic diagram is shown in Figure 3. The light source is a 484 nm argon laser with the capability of 100 mw power output. The detector was working together with a lock-in amplifier to eliminate stray light and the ambient background light, because the detector worked under outdoor open



atmosphere conditions, and the signals from the scattered source were very weak compared to daylight. The scattered light intensity was recorded by a laptop computer with 0.5 to 1 degree increment along the scattering angle from 0° up to 15° . A typical

Figure 3 Schematic diagram of light scattering experiment measured scattered light profile is shown in Figure 4.

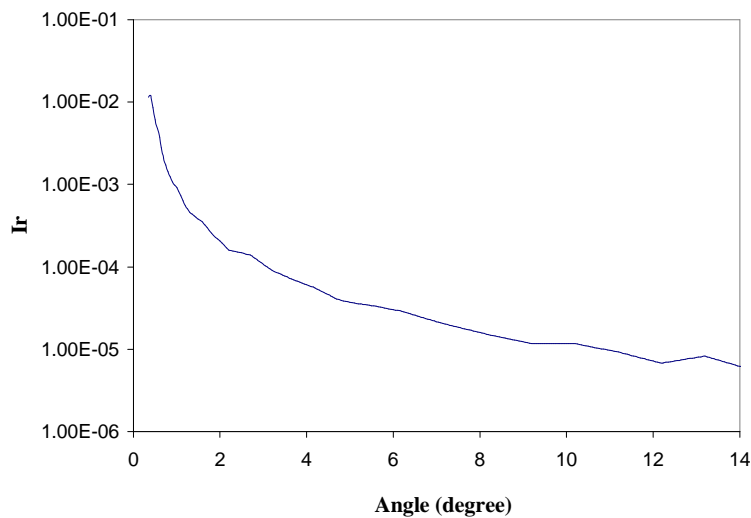


Figure 4 Scattered light profile of diesel exhaust

4. CALCULATION METHODS TO OBTAIN $N(a_i)$

There are no analytical solutions for equations (5). Either additional conditions are introduced, or numerical calculation is used to solve those equations. The first method was used is First Dark Ring (FDR) method. The second one is a numerical method to solve the nonlinear equations.

4.1 THE FDR METHOD

The FDR method requires additional information to calculate the particle size distribution $N(a)$ from equation (4). In this section, the features of the scattered light pattern of a single particle are analysed and used in the calculation for $N(a)$. The pattern of scattered light intensity of a particle is expressed by equation (2). The intensity of the scattered light varies with scattering angles.

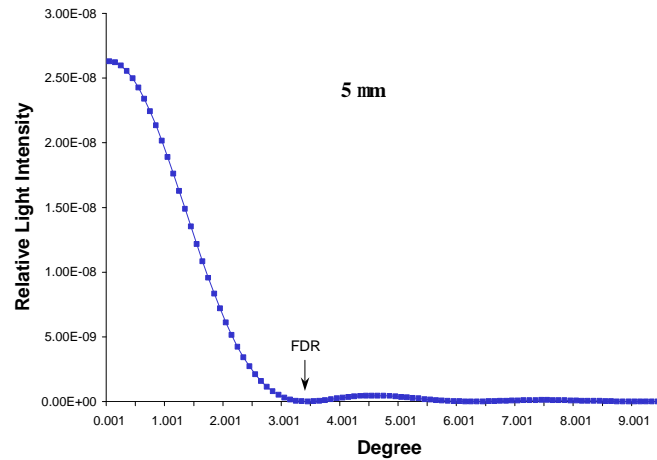


Figure 5 Scattering pattern of a single particle

When the light intensity is high, it appears bright and forms a bright ring. When the light intensity is low, it is dark, and forms a dark ring. Figure 5 shows the scattered light pattern of a 5 μm particle as an example. However, at the first dark ring, the radius a of a particle and the scattering angle q_d of its FDR follow

$$a = \frac{3.83\lambda}{2p \sin q_d}. \quad (6)$$

We assume that the intensity of the scattered light of a particle at $q < q_d$ comparing with that within the FDR can be neglected. Based on this assumption, an algorithm for calculating particle size distribution $N(a)$ is outlined as follows:

1. The smallest identified radius a_0 of the particles is determined by the scattered angle q_0 , from where $s(q)$ becomes constant or "0".
2. Set the radius increment Δa of particles, so the next considered particle size is

$$a_1 = a_0 + \Delta a.$$
3. The FDR of particle a_1 is at

$$q_1 = \sin^{-1}\left(\frac{3.83\lambda}{2pa_1}\right).$$

4. The number of particles a_0 , N_0 can be calculated from the measured signal, since the scattered light intensity at q_1 is contributed by particles a_0 according to the assumption. Therefore,

$$N_0 = \frac{s(q_1)}{I_r(a_0, q_1)}.$$

5. N_1 can be calculated at q_2 , the FDR of particle a_2 :

$$N_1 = \frac{s(q_2) - N_0 I_r(a_0, q_2)}{I_r(a_1, q_2)}.$$

6. So, for particle a_i ,

$$a_i = a_{i-1} + \Delta a,$$

and

$$q_i = \sin^{-1}\left(\frac{3.83l}{2pa_i}\right),$$

then

$$N_i = \frac{s(q_{i+1}) - \sum_{k=0}^{i-1} N_k I_k(a_k, q_{i+1})}{I_r(a_i, q_{i+1})}.$$

$N(a)$ will be obtained, when the calculation along $s(q)$ is completed. The calculations involved in this algorithm are very easy, and can be carried out by several commonly used Microsoft-Windows programmes. However this method overestimates small particles because the assumption neglects the scattered light intensity after the FDR. So the scattered light intensity after the FDR of each particle would be collected by the smaller particles.

The result by using this method will be presented and discussed in Results and Discussion Section.

4.2 THE LEAST-SQUARES METHOD

To avoid the assumption stated in the last section, the nonlinear equations (5) at the measurement points $s(q_i)$ should be used. Since the analytical solutions could not be calculated, we have to use numerical methods to solve the set of nonlinear equations.

In equations (5), both particle size a_i and particle number N_i are variables. If there were K bins in our particle size distributions, we would have $2K$ of variables, and in theory, $2K$ data points would be needed to solve the equations.

The numerical method we use is for optimisation problems, which is one of the commonly used methods to solve nonlinear equations (See reference [13]). The type of the function we targeted for optimisation is nonlinear least-squares. The objective function for calculation is the sum of squares of nonlinear equations. The principle of this calculation is to reduce the differences between measured values of scattered light and the values of scattered light produced by the estimated particle distributions. So, in this practice, our optimisation is a minimisation problem. It has the form of:

$$\min F(y) = \min \left\{ \sum_{j=1}^m f_j^2(y) \right\} \quad (6)$$

where $y = (y_1, y_2, \dots, y_n)^T$, and $m > n$. n is the number of variables, and m is the number of equations.

Rewrite equations (5),

$$s(\mathbf{q}_j) - I_q = s(\mathbf{q}_j) - \sum_i I_r(\mathbf{a}_i, \mathbf{q}_j) \cdot N(\mathbf{a}_i), \quad j = 1, 2, \dots, m.$$

The function in equation (6) becomes

$$f_j(y) = s(\mathbf{q}_j) - I_q = s(\mathbf{q}_j) - \sum_i^K I_r(y_i, \mathbf{q}_j) \cdot y_{K+i}, \quad j = 1, 2, \dots, m.$$

and

$$F(y) = \sum_{j=1}^m [s(\mathbf{q}_j) - \sum_i^K I_r(y_i, \mathbf{q}_j) \cdot y_{K+i}]^2.$$

The value of m depends on the measured data points, and K is the number of size groups (or bins) in the estimated size distribution calculated. In our case, $n = 2K$.

The numerical calculation programme codes in FORTRAN produced by Numerical Algorithms Group (NAG) were used to carry out the calculations.

The least-squares method can avoid overestimating small particles when calculating the size distributions. However, how detailed (how many sizes) size distributions that can be achieved are limited by the number of data points obtained from light scattering experiments, and the more size groups (size bins) were in the function, the longer calculating time it would need to reach a solution.

5. RESULTS AND DISCUSSION

Experiments of the light scattering from diesel particles were carried out on the facility described in section 3.3. The scattered light signals were measured from 0° up to 15° by sweeping the detector arm along the angles. The movements involved in the light scattering measurements required precision, but the environment close to the engine was very noisy with vibration. It was a very delicate operation, requiring a great deal of preparation and patience to get a reasonable scattered light profile.

The scattered light profile obtained with an engine speed 2000rpm shown in Figure 4 was used in these two different calculation methods for this paper. The results of these two calculation methods were compared with the size distribution obtained by microscopy. In order to carry out this comparison, diesel exhaust samples were taken by putting clean microscope slides into the exhaust plume while the scattered light measurement was carried out. The sample slides were prepared and gold coated, then studied in a Scanning Electron Microscope (SEM). Images taken by SEM were analysed by an image processing computer programme. The size of particles on the slides was measured, the number of particles was counted, and the size distribution was produced by the programme. Figure 6 shows the particle size distribution on the diesel particle sample slide. The two calculation methods

discussed above were used to calculate particle size distributions from the same scattered light profile. The results from the calculations and from SEM image analysis are shown in Table 1

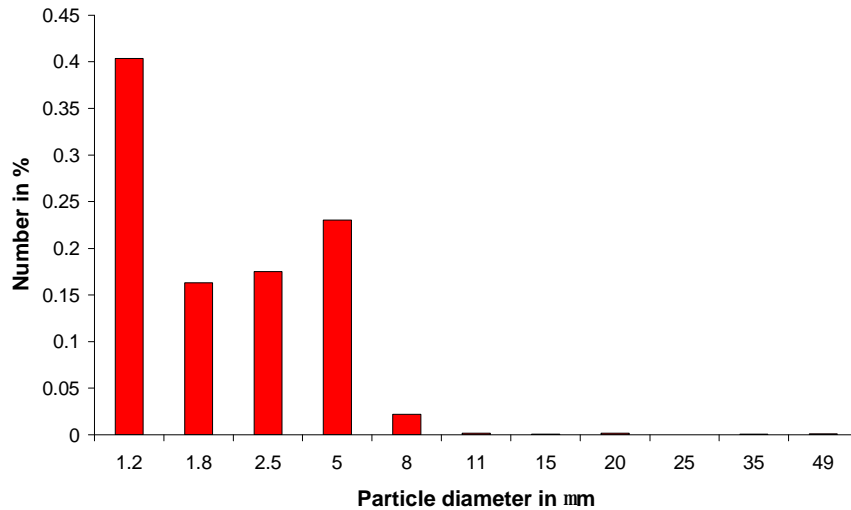


Figure 6 Particle size distribution from SEM image

In Table 1, the data under SEM, are from the SEM image; the data under FDR are the result calculated by FDR method, and those under Least-squares are the result obtained by least-squares numerical calculation. The size expressed in the table is

Table 1

SEM		FDR		Least-squares	
Size	N%	Size	N%	Size	N%
1.2	40.36627242	1.21	90.26760589	1.753	80.43656566
1.8	16.2914918	3.28	7.335034995	3.545	13.37774707
2.5	17.51239985	5.36	0.124467855	6.384	0.7752288
5	23.04463945	7.43	1.429576449	8.533	2.253247294
8	2.174742465	9.49	0	12.749	1.695145625
11	0.190766883	11.56	0	20.284	0.931713271
15	0.076306753	13.63	0.226838156	40.315	0.530352282
20	0.152613506	15.7	0.090194098		
25	0	17.7	0		
35	0.076306753	19.8	0		
49	0.11446013	21.9	0.52628256		

the diameter of particles, in *mm*. The number of particles at each size range is presented in percentage to the total number of particles.

All of the three data sets in Table 1 show that most of the particles from the diesel

exhaust are small particles, < 2.5 *mm*, and very small amount of relatively large particles, no larger than 50 *mm*.

In the smaller size range, e.g. under 1.8 *mm*, nearly 60% of the particles were counted from the SEM image; the Least-squares result shows about 80% in this range, while the result from FDR is over 90% at 1.21 *mm* only. As it was predicted before, the FDR method would over estimated small particles, and it does not show any particles larger than 25 *mm*, but both SEM image and Least-squares results show the occasional large particles present in the diesel sample.

The SEM image shows there is a small peak, more than 20% at near 5 *mm* regions in its size distribution. Both of the calculated results do not have this peak in a similar

region. The Least-squares result shows a small increase at about 8 μm and the FDR result has an even weaker increase at near 7 μm .

Figure 7 shows the same sets of results in accumulative distributions. All three results have the same trend of the size distribution. Overall, Least-squares result is closer to that derived from the SEM image than FDR result. The proportion of small particles in FDR result is clearly more than those in the others.

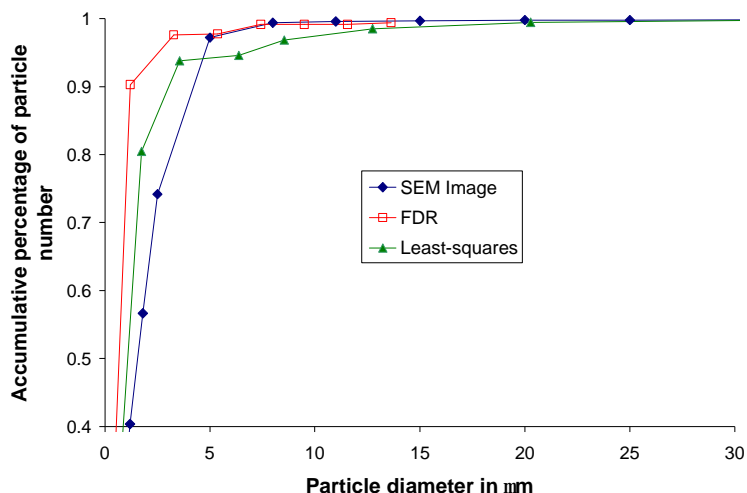


Figure 7 Comparison of accumulative percentages of particle number

Seven size groups were the best choice we could do with the Least-squares method due to the number of experimental data points. The limit of choices of particle sizes made the approach to the real distribution less easy than it

could have been. Apart from this weakness of Less-squares' calculation and the additional assumption made in the FDR method, there is a common aspect for those two calculations not to have same detailed features in the size distributions as the SEM image, that is the accuracy of scattered light signal measurements in the relative large angle range. The difference between the signal levels from a small angle to a relatively large angle, $> 10^\circ$, was more than 10,000 times. A single detector system could not keep the same sensitivity within such a large range of the signal level. The signals measured in the large angle range had a relatively high noise level, which directly affected the results for small particles particularly. However, the light scattering method has shown encouraging results, and to increase the accuracy of scattered light measurements, the experimental system requires improvements.

Seven size groups were the best choice we could do with the Least-squares method due to the number of experimental data points. The limit of choices of particle sizes made the approach to the real distribution less easy than it could have been. Apart from this weakness of Less-squares' calculation and the additional assumption made in the FDR method, there is a common aspect for those two calculations not to have same detailed features in the size distributions as the SEM image, that is the accuracy of scattered light signal measurements in the relative large angle range. The difference between the signal levels from a small angle to a relatively large angle, $> 10^\circ$, was more than 10,000 times. A single detector system could not keep the same sensitivity within such a large range of the signal level. The signals measured in the large angle range had a relatively high noise level, which directly affected the results for small particles particularly. However, the light scattering method has shown encouraging results, and to increase the accuracy of scattered light measurements, the experimental system requires improvements.

6. IMPROVEMENT IN EXPERIMENT AND FUTURE WORKS

The following improvements in the experimental system have been made:

- A multi-detector system has been designed, so all of the scattered signals can be recorded at the same time. Unexpected disturbance from the background can be limited, and instantaneous measurements can be carried out easily.
- Lenses are used for each detector to increase the scattered light intensity. In particular, the quality of scattered light signals in the large angle region has been significantly improved [11].
- A multi-channel lock-in amplifier and synchronised data controller system is used.

The improved system, which is shown in Figure 8, is more robust than the previous one. Light scattering experiments with running engine can be carried out easily and quickly. The scattered light from every angle can be recorded at same time. It is a real-time spontaneous measurement. This system is one step closer to a real-world vehicle testing system

Since the system of the measurements of light scattering has been changed, the quality of signals has been greatly improved. Unfortunately as a consequence of using lenses the number of data points is less than before, as a lens covers a range of scattering angles. The objective function in the method to solve non-linear equations will therefore have to be changed. Other numerical methods rather than the Least-squares method will be analysed and tested, since the Least-squares method is no longer appropriate to solve size distributions from the data obtained from the new signal collecting system.



Figure 8 The improved system

A more comprehensive diesel particle model should also be investigated. The shape factor as well as the finer particles should be considered in future models. The sizes of the finer particles are comparable to the wavelength of the incident light.

In the future, the appropriate numerical method and a comprehensive particle model will form a new software package. Once the scattered light of particles from an exhaust pipe is recorded, this software will produce the size distribution. So the experiments with different diesel engines, under different operational conditions can be undertaken. In particular, the capability of the light scattering method to measure particle sizes during engine's transient operations should be assessed.

7. ACKNOWLEDGEMENTS

Funding assistance from the Public Good Science Fund of the New Zealand Government is gratefully acknowledged. Beaglehole Instrument designed and built the multi-channel lock-in amplifier system to improve the quality of the experiments.

8. REFERENCES

1. National Center for Environmental Assessment Office of Research and Development, 'Health Assessment Document for Diesel Engine Exhaust', *EPA/600/8-90/057F*, May 2002
2. Chambellan, A, Crestani, B, Soler P., Moreau, J., Aubier, M., 'Diesel Particles and Allergy: Cellular Mechanisms', *Allerg Immunol (Paris)*, 2000, Feb. 32(2):43-8, Unique identifier: AIDSLINE MED/20203076.
3. Smith, R.; Davis, J.M.; Sacks, J.; Speckman, P.; Styer, P. *Environmentrics* 2000, 11, 719-743
4. Michaels, R.A.; Kleinman, M.T. *Aerosol Sci. Technol.* 2000, 32, 93-105

5. Seethaler R. 'Economic Costs of Air Pollution-related Health Impacts - an Impact Assessment Project of Austria, France and Switzerland', *Proceedings of 16th International Clean Air and Environment Conference of the Clean Air Society of Australia & New Zealand*, Christchurch, New Zealand, 19-22 August 2002.
6. Lammel, G.; Novakov, T., 'Water Nucleation Properties of Carbon Black and Diesel Soot Particles', *Atmospheric Environment*, 1995, 29, (7), 813-823
7. Levy, D., 'Diesel Soot Added to List of Global Warming Culprits', *Stanford Report*, Dec. 12, 2001
8. Cadle, S.H.; Gorse, R.A.; Bailey, B.K. and Lawson, D.R., 'Real-World Vehicle Emissions: A Summary of the 10th Coordinating Research Council On-road Vehicle Emissions Workshop', ISSN 1047-3289 *Journal of the Air & Waste management Association*, 2001, 51:236-249
9. Moosmüller, H.; Arnott, W.P.; Rogers, C.F., et al, 'Time Resolved Characterization of Diesel Particulate Emissions. 1. Instruments for Particle Mass Measurements', *Environmental Science & Technology*, 2001, 35, No 4, 781-787
10. Cheung, S.K.; Elder, S.T.; Rain, R.R., 'Diesel Particulate Measurements with a Light Scattering Photometer', *SAE Technical Paper Series*, 2000-01-1136
11. Gong, R., 'Analysis of Options for Increasing the Sensitivity of a Light Scattering Method for Measuring the Size Distributions of Diesel Particulate emissions', *Proceedings of 4th World Congress on Particle Technology*, 2002, Sydney, Australia, ISBN 085 825 7947
12. van de Hulst, H.C., 'Light Scattering by Small Particles', published by John Wiley & Sons, Inc. 1962
13. NAG Manual, Fortran 77 Library, Mark 19.